# Journal of the National Academy of Forensic Engineers®


http://www.nafe.org

ISSN: 2379-3252

DOI: 10.51501/jotnafe.v39i1

Vol. 39 No. 1 June 2022

# FE Investigation and Analysis of Poor Electrical Connections and Related Fire Investigation Case Studies

*By Timothy C. Korinek, PE (NAFE 1023M)*

**Abstract**

*Overheating poor electrical connections (OPCs) are a ubiquitous ignition source of structure fires. Yet, knowledge of the intimate process between conductors at the connection point is relatively undocumented on the microscopic scale. For an OPC, it is ordinary for a filament or pool of liquid oxide to be the main current-carrying conductor at the point of overheating. This paper examines the overheating phenomena from a materials science perspective using photography through the stereo microscope, cross-sectioning, electron microscopy, and specialized techniques under the metallurgical microscope. Two case studies are presented in the second half of this paper. The first presents an artifact from field testing performed by a commercial cooking appliance manufacturer and introduces a real-world example of an OPC that did not ignite surrounding materials. The second is from a fire investigation of a food processing plant where prior research on OPCs informed expert opinions at trial and influenced the results.*

**Keywords**

Poor connections, glowing connections, electrical overheating, electrical ignition sources, liquid oxides, liquid oxide conductor, high-resistance connections, high-temperature oxidation, forensic engineering

## Background

Overheating poor connections (OPCs) are also referred to as glowing connections or high-resistance connections. These terms are often used interchangeably in the context of fire investigation. All overheating connections are, by their nature, high-resistance connections, but this paper focuses on OPCs that have some portion of the connection area glowing red-hot or higher. It aims at giving the investigator a better understanding of how a liquid oxide conductor behaves in an OPC and some unique features that can serve as evidence to prove an OPC occurred in the field. Readers are encouraged to seek out the references cited in this paper for additional information. The chapter on contacts and connections in *Electrical Fires and Explosions*[1] includes the results produced by many different investigators and is highly recommended.

The presence of liquid oxide as the stable electrical conductor at an established OPC is the predominant feature observed in the research performed by this author with currents in the range of 1 to 15 amps[2,3], and is well documented in the literature for currents ranging between 0.5 to 50 amps for various material combinations[1,4]. In the tests performed by this author — even when an OPC appears to be statically glowing — a liquid filament bridge was always observed to exist. This was determined by careful visual observation of the connection under the stereo microscope in real-time during overheating — and by metallographic cross-sectioning afterward, which reveals the existence of a formerly liquid region on top or within a larger oxide mass.

The oxide mass is sometimes referred to as the “nugget” in this paper. It consists of mostly solid oxide, but all areas of it were part of the liquid filament at some previous point in time. In many cases, the glowing liquid filament can be observed to wander around like a worm, causing further oxidation of the metal conductors and growth of the oxide mass. The liquid oxide filament is sometimes referred to as the “worm” in this paper. The worm-like action of the liquid filament is one characteristic that helps OPCs be stable for long periods of time. As the worm wanders around, it’s continuously melting and remelting regions of the oxide mass that produces a self-healing

Timothy C. Korinek, PE, N144 W6466 Pioneer Rd., Cedarburg, WI 53012, 414-791-2434, tim.korinek@efiglobal.com

effect regarding the mechanical stresses caused by thermal gradients and volume expansion from oxide growth. If there were no wandering melt zone, these stresses would tend to crack the brittle oxide and open the electrical circuit.

The types of OPCs studied in this paper involve connections between Cu-Steel, Cu-Cu, and Brass-Brass. The data in **Figure 1** outlines the materials and circuit parameters examined in this study. All of the samples researched by this author produced evidence of a liquid oxide conductor at the connection interface.

The ranges of currents (as provided in **Figure 1**) represent different electrical loads. For example, about half of the Cu-Cu AC tests employed a number of incandescent light bulbs such that the current was 1.5 amps through the connection. Additional light bulbs were added in parallel for other tests to increase the current through the connection to 2.2 amps. For every situation studied, the overheating connection did not appear to be the controlling factor of the current.

It can be convenient to think of an OPC as a high-resistance hot-spot composed of a solid material (such as a miniature Nichrome heating element), but there are some distinct differences between the two. There is also a point where this analogy fails to properly characterize what actually happens in an OPC. OPCs involve one or more oxide species as an electrical load, and these oxides have a negative temperature coefficient of resistivity (NTC)[1], whereas metals like Nichrome have a positive temperature coefficient of resistivity (PTC)[5]. For the oxide semiconductors involved in an OPC, the electrical resistance decreases with increasing temperature, which is the opposite behavior observed for metals.

At a given temperature, metallic heating elements have resistivities many orders of magnitude lower than oxides such as $Cu_2O$ (cuprous oxide). A useful chart of material resistivities is given in *Principles of Electronic Materials and Devices* [p. 130 Fig. 2.7][5]. By modeling an OPC as a resistance heating element, the overheating contact area can be as small as a thin film. The comparative difference in resistivities between a metallic heating element and an oxide can certainly be offset by the difference in lengths. Since the circuit resistance also depends on the conductor geometry, it is plausible that a very thin oxide with high resistivity can have the same resistance as a longer metal conductor with much less resistivity.

| OPC material Combination | Nominal Circuit Voltage | AWG & Wire Type, or Conductor | Number of Samples Produced | Range of Current Through the Connection (Amps) | Duration of Test[c] (minutes) |
|---|---|---|---|---|---|
| Cu-Cu | 120 V AC | 14, Solid | 28 | 1.5[a] — 2.2 | 35 — 480 |
| | | 12, Stranded | 6 | 1.6 — 2 | 40 — 450 |
| | 12 V DC | 14, Solid | 17 | 2.2 — 7.2 | 16 — 180 |
| | | 12, Stranded | 2 | 3.7—3.75 | 60 — 255 |
| Brass-Brass | 120 V AC | Plug blades | 28 | 1.5[b]—2.3 | 15—420 |
| | 12 V DC | Plug blades | 3 | 2.2—3 | 115—150 |
| Cu-(Ni plated Steel) | 120 V AC | Copper wire-Steel Terminal Screw | 50 | 12 | 20—7200 |

[a] One sample was tested at 0.5 V for 120 minutes as a low current example.

[b] Two of the tests were performed at higher currents, 9.2 Amps and 13.8 Amps.

[c] The test duration was sometimes stopped before the connection melted open. Some tests were also stopped at the end of the business day.

**Figure 1**
Table of different OPC configurations tested.

The behavior of a metallic heating element is to have the highest current upon startup when the element is cold (i.e., inrush current). After startup, the resistance increases as the element heats up (often to red or orange hot), and the circuit reaches a steady state balance between the resistive heating (aka joule heating or $I^2R$ heating) and the corresponding PTC material response.

In contrast, when an oxide with NTC behavior acts as a high-resistance element in a circuit, the resulting joule heating causes a decrease in resistance. This introduces one divergence with the analogy of the oxide as a conventional high-resistance heating element. The second divergence comes with the fact that, when an OPC glows red hot, high-temperature oxidation of the metal occurs next to (and at) the connection interface. For the copper oxides at temperatures above 300°C, the rate of high-temperature oxidation growth is parabolic with respect to time[6].

If the oxide conductor is modeled as existing only as a solid, the basic materials behavior described above has important implications on how an OPC develops in a real-world application. It is apparent that any significant overheating that takes place at the interface may also be in competition with an oxide thickness increase, which would increase the connection resistance and decrease the overheating wattage. If the effects of the NTC behavior upon heating predominate over any thickness increase, then it is possible a connection will proceed in "run-away" heating, which can cause the oxide layer to melt[1]. This behavior may explain why OPCs can sometimes be re-initiated again after being separated[7]. Experiments have shown the molten oxide has an additional order of magnitude drop in electrical resistance associated with the phase change from solid to liquid[1].

For the OPC samples prepared in the lab by this author, the method of initiating the OPC was by establishing the molten oxide worm by causing series micro-arcing, after which the worm starts out as a very small-sized ball or bridge. Much attention has been given to vibrations as a means to initiate micro-arcing. However, even at small currents, the high local temperatures created from one or a few micro arcs can be sufficient to establish the molten oxide worm. In fact, it has been the experience of this author that it is easier to initiate an OPC by separating the current-carrying conductors ultra slowly, compared to repeated vibratory micro-arcing. For example, this author employed a small DC motor with an eccentric weight (such as a cell phone ringer), which was used to cause vibrations and continued micro-arcing. When the vibratory motor was used to attempt OPC initiation, it was sometimes very difficult and took many hours to start an OPC, especially with direct current OPCs.

This author also employed a rack and pinion fixture with one moveable contact. With a little practice, it was easy to get all types of the studied OPCs to initiate by lightly "kissing off" the conductors with the rack and pinion fixture. It took some practice with the rack and pinion fixture to make the motion small enough, but this method was observed to initiate OPCs far easier than a condition subjected to regular vibrations. This same mode of initiating an OPC is reported in *Electrical Fires and Explosions*[1] and is described as "extremely low separation of the contacts," where the researchers used controlled thermal contraction as a means to slowly separate a connection.

## Aspects of How OPCs Can Occur

It's well known that light contact is the main prerequisite to OPCs[1]. There are many routes by which this can happen in a real-life circumstance. Below is a list of some scenarios that may be causative of an OPC. This list is not exhaustive, and many of the factors can also be interrelated or exist in combination.

1. Aside from thermal run-away of an overheating solid oxide layer, the remainder of the causative conditions are due to series micro-arcing as the OPC initiator.

2. Oxidation at or next to the connection interface from any source, such as high-temperature oxidation or aqueous corrosion. An accelerated scale or medium that causes a mechanical separation and a decrease in metallic contact area (and eventual separation of the contacts) can cause parting micro-arcing. The Pilling-Bedworth (PB) ratio compares the volume of an oxide with its corresponding metal. Most metal oxides have a PB ratio greater than 1, which means the volume of the oxide is greater than the metal. $Cu_2O$ has a PB ratio of 1.67[8]. When the copper oxide layer is formed on a copper substrate, a mechanical volume expansion occurs that can separate conductors previously in contact. The nature of a liquid conductor also provides an extra degree of freedom considering the electrical circuit. Reference 1 shows how the worm size is affected by the current density on a Cu-Cu OPC.

3. Stress relaxation of spring elements that make

connections, such as receptacles. Spring elements made from copper and copper alloys are known to relax over time under stress[9]. External stresses from either normal or abnormal use can exacerbate these effects.

4. Environmental conditions, such as thermal expansion and contraction from temperature changes, can influence a loose connection.

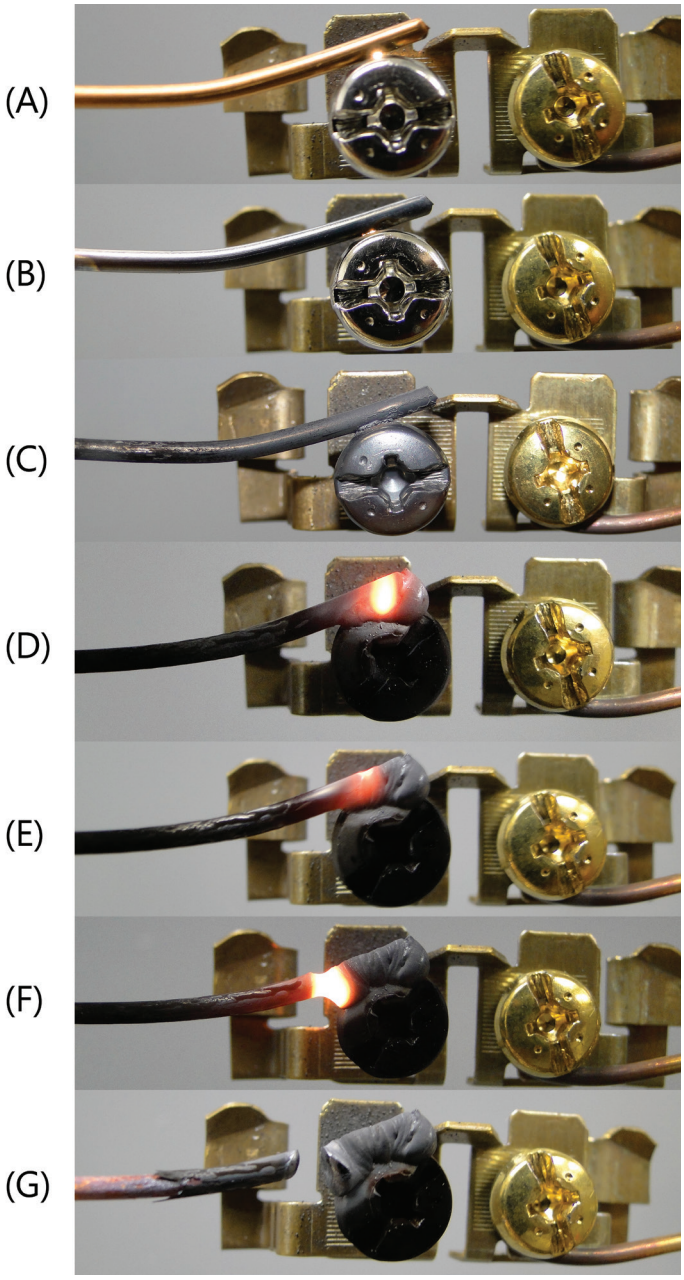


**Figure 2**
Common sequence of overheating for a loose connection between copper and steel, such as an improperly tightened wire on a receptacle screw terminal.

5. Installation error, misuse, normal wear, abuse while in service, or design defects that result in unnecessary connection looseness should all be considered when evaluating a possible OPC.

**Figure 2** shows a time lapse sequence of an OPC produced in the lab between a 14-gauge solid copper wire and a nickel-plated steel screw with 12 amps of current running through the connection. These photos were taken as part of the research presented in "Pre- and Post-Flashover Characteristics of an Electrically Overheated Poor Connection Between Copper and Steel"[2]. This connection is ordinarily made by wrapping the wire around the shaft of the screw resembling a pig-tail, but the configuration of a wire simply in contact with the top of the screw was chosen to bring the overheating features into full view.

In many common scenarios, such as plug-blade receptacle connections or crimp terminals, the actual connection interface is hidden out of sight, making it difficult to demonstrate what occurs inside of an overheating connection. Research in "Electrical Receptacles - Overheating, Arcing, and Melting,"[10] used the same connection materials and similar circuit conditions as **Figure 1**. They used a pigtail configuration and produced OPCs that have identical features (except the oxide nugget assumes the shape of the pigtail). This is consistent with the observations of this author that the remnants of an OPC often are a function of the original connection geometry, but the essential characteristics of why the overheating happened (and what evidence is left behind) are the same.

**Figure 2(A)** shows micro-arcing at the contact point caused by manually making and breaking the contact. The OPC can be initiated with as little as one light touch. Soon after, a ball of molten oxide is established in series with the circuit, and significant heating of the surrounding conductors begins.

**Figure 2(B)** shows the OPC within minutes of establishment of the molten oxide. The copper wire has now darkened because a layer of adjacent oxide has formed. This layer is caused by high-temperature oxidation and is a secondary effect of the heating taking place at the contact point. The secondary high-temperature oxidation is a solid-state process.

**Figure 2(C)** displays the appearance of the OPC on the order of several hours after initiation. A nugget of oxide about the size of a grain of rice exists at the interface between the wire and screw. At this stage, the wire

sometimes glows red-hot due to the heating taking place at the connection point. The molten oxide also glows, but is not always visible when viewing the connection from the exterior because the liquid filament is inside the nugget. As the oxide mass at the connection point grows, the liquid path is often a fraction of the entire mass. It will wander around, re-melting formerly molten areas. The thickness of the secondary high-temperature oxide layer has also thickened over time, and the screw is beginning to show secondary high-temperature oxidation on the surfaces away from the connection point. The OPC can stay in this stage for a considerable amount of time before transitioning to (D), if at all. As emphasized throughout this paper, the geometry and circuit conditions can influence the form an OPC will take.

**Figure 2(D)** shows the stage in which the oxide nugget has grown to the point where the molten pool is large, and more than half of the wire nearest to the connection point has been converted to oxide. The bright yellow area is the molten region. A needle or probe can easily be inserted into the molten pool without it dripping due to the surface tension.

**Figure 2(E)** shows the molten pool wandering at a later stage. More of the wire and screw have been converted into oxide due to the molten pool. For the copper-to-steel connections studied at 12 amps, more of the copper wire was converted to oxide compared to the iron from the screw. In addition, it took between 10 and 100 hours of runtime to reach the stage shown in (F).

**Figure 2(F)** shows the molten pool, which is only supported by surface tension in this stage, but still conducting all of the circuit current.

**Figure 2(G)** shows the connection after it melted open.

The scanning electron microscope (SEM) image in **Figure 3** shows a mounted and polished longitudinal cross-section through a sample in a state comparable to **Figure 2(C)**, where the oxide nugget is about the size of a grain of rice. This image was taken with a backscattered electron detector (BSE), which produces a grayscale contrast based primarily on the local atomic weight of the sample regions. Higher atomic weight results in lighter shades, and lower atomic weight will have darker shades. The copper wire is the brightest; the dark background is the epoxy mounting material. The red arrow points to the formerly liquid oxide nugget between the wire and screw, and the blue arrow points to the secondary high-temperature oxide growth layer. This sample was stopped after 107 hours of overheating.

**Figure 4** shows the secondary high-temperature oxidation of a copper wire in greater detail. This image is an unmounted cross-section of the oxide layers after some of it fractured away. The oxide is a dual layer composed of $Cu_2O$ grown at the Cu metal interface, and CuO grows on top of the $Cu_2O$. The ratio of $Cu_2O$ to CuO thickness is dependent on temperature[6]. The CuO grows into the atmosphere as whiskers, which would resemble something like a winding staircase on the atomic level. The whiskers then coalesce into a polycrystalline CuO layer with the $Cu_2O$ underneath. For the time and temperatures of the Cu-Cu

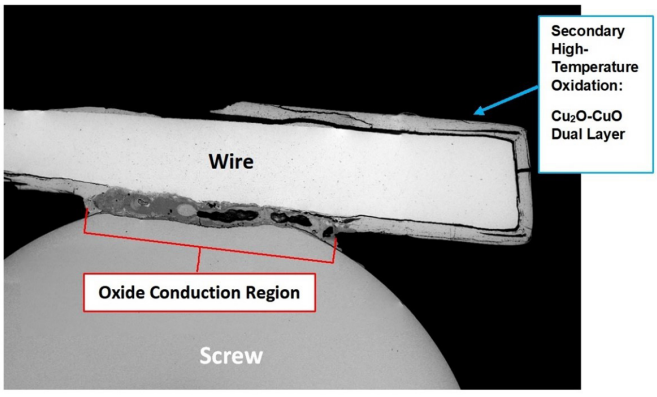


**Figure 3**
Mounted and polished cross-section[2] showing the overheating interface between a loose wire making contact with a steel screw. Evidence of the worm is not always found in a cross-section because it is only a single two-dimensional slice — the worm can be in a different location.

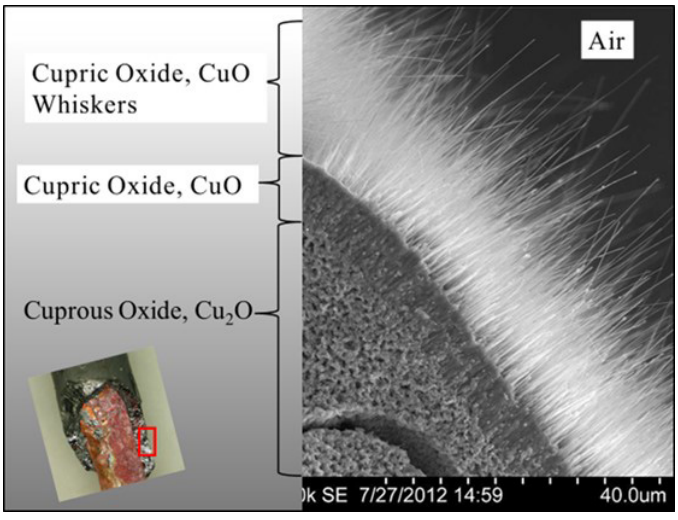


**Figure 4**
SEM image showing the dual copper oxide scale plus the whisker morphology of the outer layer after high temperature growth[2].

OPCs studied, the $Cu_2O$ layer predominates in thickness. For those readers who are only familiar with aqueous electrochemical oxidation of metals (usually referred to as corrosion), the mechanism of dry high-temperature oxidation is different — but not entirely. With aqueous corrosion, the chemical reactions take place via ionic conduction of dissociated species through an electrolyte. High-temperature oxidation still involves species with an effective charge, but the transport takes place via electronic conduction through the layer, such as with positively charged holes and vacancies in the crystal.

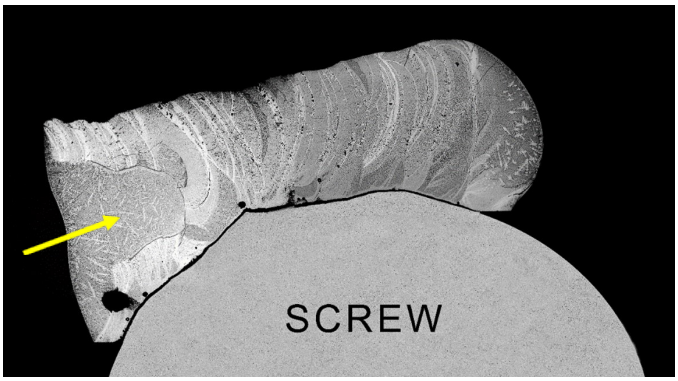


**Figure 5**
An as-polished metallurgical cross section[2] of an OPC remnant from a connection between a 14-gauge copper wire and a steel screw as shown in **Figure 2**. All parts of the wire in the vicinity of the screw have been part of the molten oxide worm at some point, and the region that was molten immediately prior to the connection melting open is the bell-shaped feature on the left-hand side (as indicated by the yellow arrow).

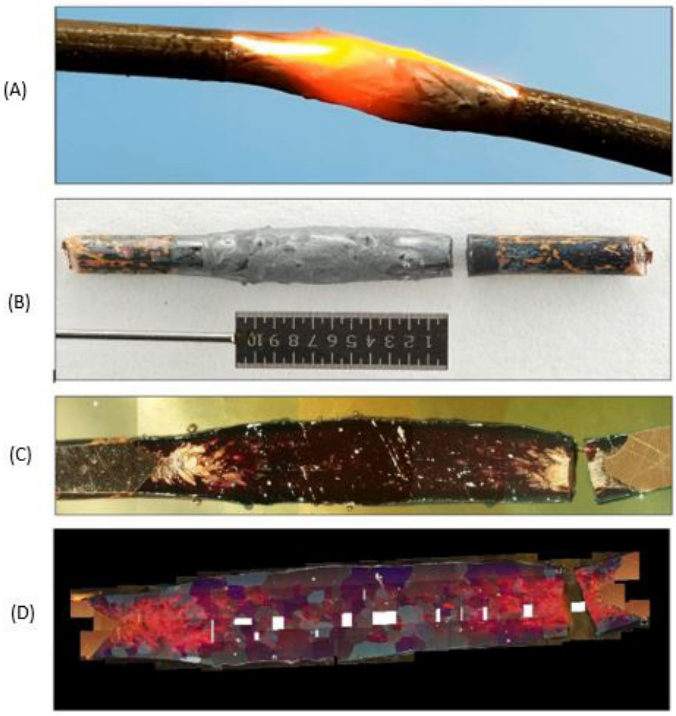


**Figure 6**
A Cu-Cu OPC showing (A) the worm and oxide nugget growth after a period of overheating, (B) remnants after shutting the circuit off, (C) as-polished cross section of the connection with incident lighting under the stereo microscope, and (D) composite image of photos taken with the metallurgical microscope using crossed polarizing filters[3].

**Figure 5** is a SEM-BSE image, and shows the sample from **Figure 2(G)** after being mounted in epoxy and polished to achieve a cross-section. There is no evidence of any melted copper wire or melted steel. The species that were molten consist entirely of copper-oxides and copper-iron-oxides[2]. Despite these observations, it is possible for melting of the metallic conductors to take place (this will be discussed later in the paper).

**Figure 6** shows a copper-to-copper OPC produced in the lab with 1.6 amps of current flowing[3]. After the overheating connection is established, the liquid filament acts like a worm that wanders through the already-oxidized mass. The liquid oxide is stable on a time frame of minutes to hours, and there is a self-healing effect of the worm wandering around — melting and remelting — which helps sustain the process and keeps the connection intact.

**Figure 6(A)** shows a photograph of the molten worm and oxide mass during the experiment, which exists as a bridge more than 1 cm long after 4 hours of overheating since the OPC was initiated.

**Figure 6(B)** shows the sample after the circuit was shut off. When the circuit was shut off, the sample cooled and fractured, which can be seen on the right-hand side of the photo. The scale shown in the photo is 1 cm total in length, and the numbered divisions are millimeters.

**Figure 6(C)** shows the same sample mounted and polished longitudinally, viewed under the stereo microscope.

**Figure 6(D)** is a composite image of more than 100 long-exposure photos taken through the metallurgical microscope using completely crossed polarizing filters and stitched together afterward. The exposure time for each photograph was approximately 30 seconds. With completely crossed polarizers, the field of view when framing these shots is completely dark. The filters are not perfect materials (or perfectly crossed), so some light gets through, resulting in the images shown. The white areas in the image compilation were missed areas because it was difficult to know where the shot was before taking it.

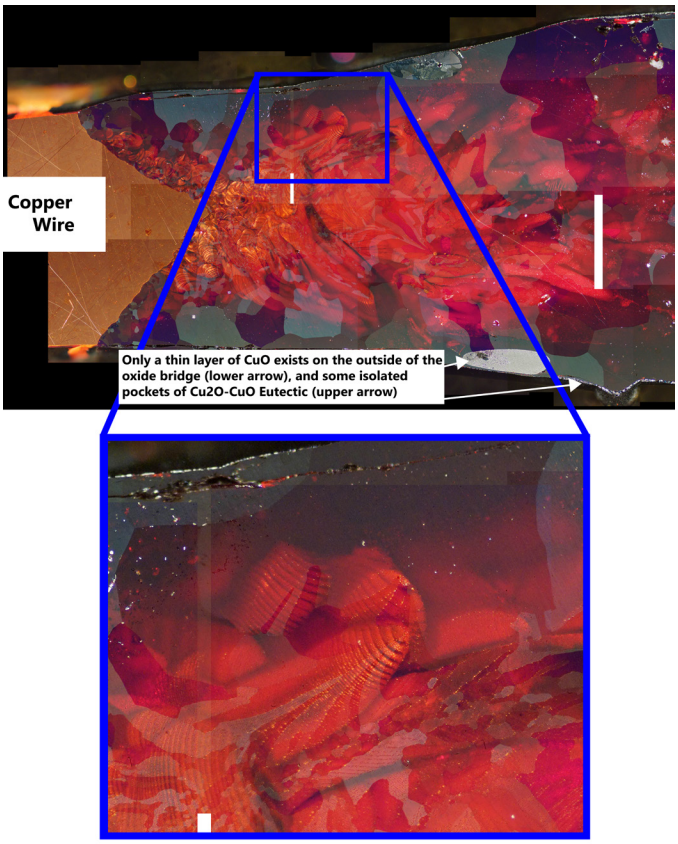


**Figure 7**
Images from **Figure 6(D)** at higher digital zoom. There is a thin outer layer of CuO and some pockets of $Cu_2O$-CuO eutectic, as indicated by the white arrows. The segmented morphology of the worm microstructure is apparent[3].

Cuprous oxide ($Cu_2O$) is a semitransparent material, so the photos also display features inside the cross-section below the plane of polish. $Cu_2O$ also shows up as red colored under the microscope when using polarized filters[11].

**Figure 7** shows the left-hand region from **Figure 6(D)** at a higher magnification. The microstructure of the worm can be seen; it actually represents many past locations of the worm. One aspect to reiterate is that $Cu_2O$ is semitransparent, and using crossed polarizing filters allows features below the plane of polish to be observed — so some areas inside the material can be seen. It is also important to note that only a thin layer of CuO is found on the outside of the nugget, except for a few small pockets containing $Cu_2O$-CuO eutectic. This is also consistent with the dual layer discussed earlier. The cross-section is useful because if only energy dispersive spectroscopy (EDS) were to be performed non-destructively on the surface of the nugget, one could come to the incorrect conclusion that the whole nugget is composed of CuO.

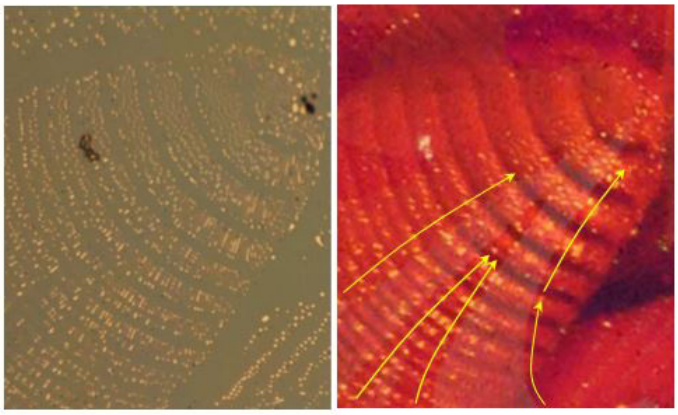

**Figure 8**
Image of the worm microstructure with normal brightfield reflected illumination under the metallurgical microscope (left); the copper globules are peach colored, and the $Cu_2O$ matrix is gray and opaque. Same region of the worm under crossed polarizing filters with long camera exposure time (right); the copper globules are gold colored, and the $Cu_2O$ matrix is red and translucent, which shows additional copper globules below the surface and surface macro grain morphology (as shown by the yellow arrows)[3].

**Figure 8** shows a comparison of the worm microstructure with different illumination techniques under the metallurgical microscope. One interesting aspect of this microstructure is that it displays banding and segmentation similar to an earthworm. The cause for this morphology deserves more research. While the glowing oxide worm from the outside looks visually similar for many OPCs between different materials (including both AC and DC currents), the microstructure of the worms in the plurality of scenarios has yet to be studied in greater detail and deserves more research.

A temperature-composition equilibrium phase diagram of the copper-oxygen system is shown in **Figure 9**, which is from "Critical Assessment and Thermodynamic Modeling of the Cu–O and Cu–O–S Systems,"[12] and some additional overlays have been provided by this author to show the Cu-Cu OPC situation. Additional thermodynamic data for the Cu-O system can be found in *Phase Diagrams of Ternary Copper-Oxygen-Metal Systems*[13].

Beside the temperature and composition of the elements involved, oxygen pressure isobars are included. A value of 0.21 atmospheres (atm) represents air (i.e., 21% oxygen). The 0.21 atm line in the phase diagram is shown by the highlighted labels in red, and the rest of the isobars are shown in terms of $\log_{10}(P(O_2)$, in atm. The melting point at (E) in **Figure 9** for the two-phase region consisting of $Cu_2O$+CuO is about 1,125°C in an ambient 21% oxygen environment.

The vertical blue line indicates the stoichiometric $Cu_2O$ compound at 33% atomic oxygen concentration. The congruent melting, which occurs at (C) at 1,231°C, is commonly cited as the melting temperature for copper oxide. Yet, care must be taken when interpreting the phase diagram. The kinetics (i.e., rate) of a particular reaction are also not represented at all in the phase diagram — as well as the fact that the partial pressure of oxygen will not be 0.21 atm. inside the oxide.

The molten L1 + L2 region in **Figure 9**, as highlighted in yellow, shows the compositional region relating to the worm. The worm involves a copper-rich L1 and liquid oxide L2. Below the critical point at (G) is a miscibility gap region below which liquid copper and liquid oxide exist analogous to oil and water at room temperature, and the solid structure upon cooling creates the microstructure of the worm. This is part of the monotectic transformation resulting in solid Cu + $Cu_2O$. The monotectic reaction is bounded by the two regions labeled (B) in **Figure 9**.

As mentioned earlier, the kinetics of the reaction are also important and not represented in the thermodynamic phase diagram. The red highlighted path in **Figure 9** shows how the 0.21 atm. isobar can be followed down the diagram to predict which substance is stable at a given temperature at a constant $P(O_2)$. In fact, the thermodynamic phase diagram dictates that CuO is the stable phase at ambient conditions (room temperature and oxygen partial pressure of 0.21 atmospheres). The diagram predicts metallic copper is not stable and should transform to CuO. The reality is that the kinetics of this reaction can be so slow that it's often not practical to consider. For example, metallic copper lasts on earth for thousands of years under

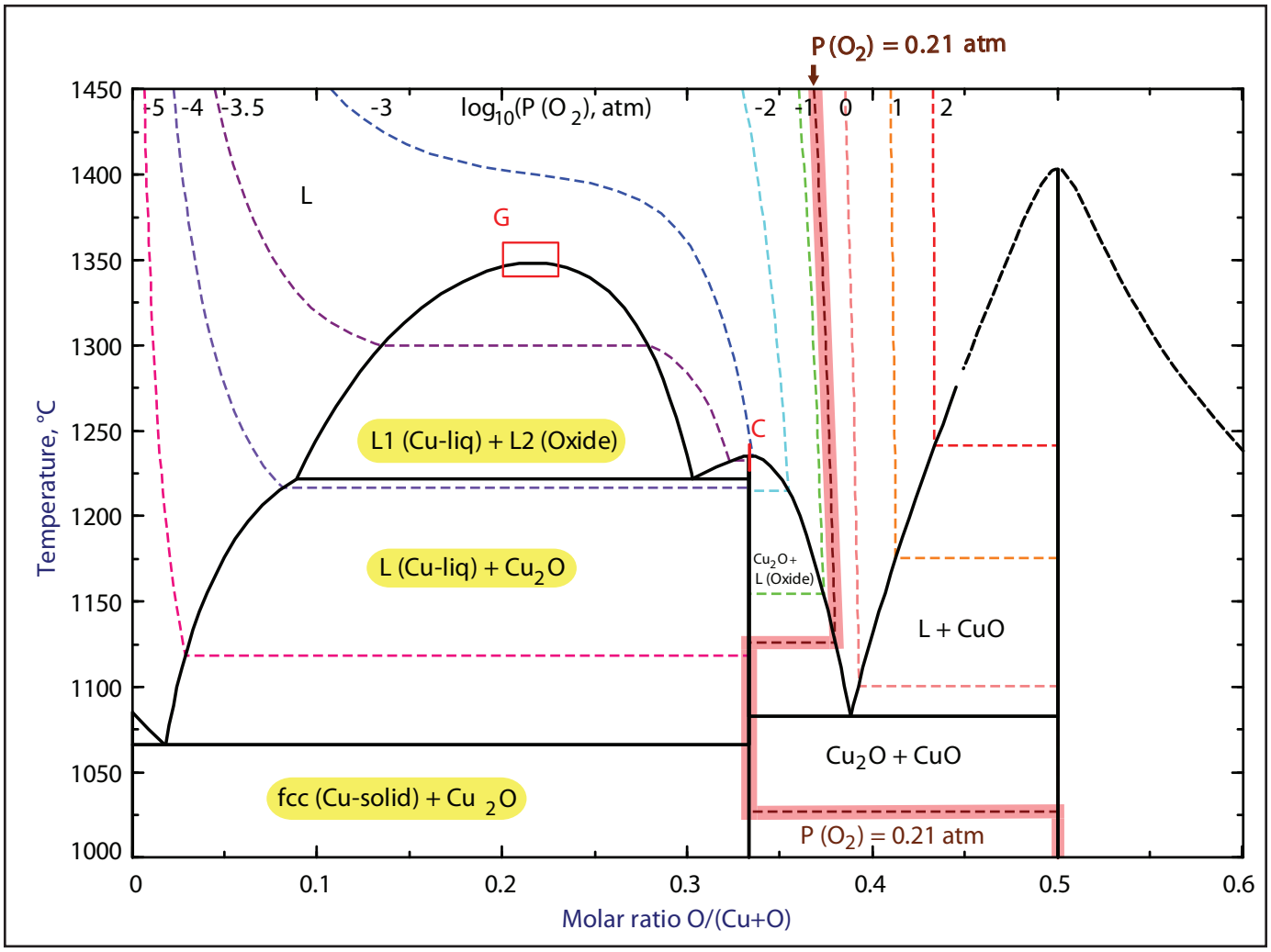


**Figure 9**
Phase diagram of the copper oxygen system with oxygen pressure isobars. The diagram was produced by the researchers in "Critical Assessment and Thermodynamic Modeling of the Cu–O and Cu–O–S Systems,"[12] and used the software program FactSage to generate the chart from available thermodynamic equations. The red and yellow highlights are overlays added by this author.

standard conditions (aqueous corrosion aside).

Nevertheless, the partial pressure of oxygen $P(O_2)$ is useful for predicting many reactions, and a three-dimensional oxide layer will be subject to a gradient of $P(O_2)$, depending on the depth. The partial pressure of oxygen decreases with depth into the solid layer, as shown in **Figure 10**[15]. This fact is consistent with the microstructure of the Cu-Cu OPC nugget, worm, and the dual scale phenomena for high-temperature oxidation of copper in air.

**Figure 11 (A)** shows an OPC with 12-volt DC with an overheating connection running 6 amps of current after several hours of overheating time. Note that with a DC current, the nugget only grows in the direction of the positive anode. This behavior is rather unusual in terms of basic heat transfer and may relate to the semiconductor nature of the oxide. More research is warranted in this regard. The unidirectional growth of the oxide nugget has been noted by other researchers[1].

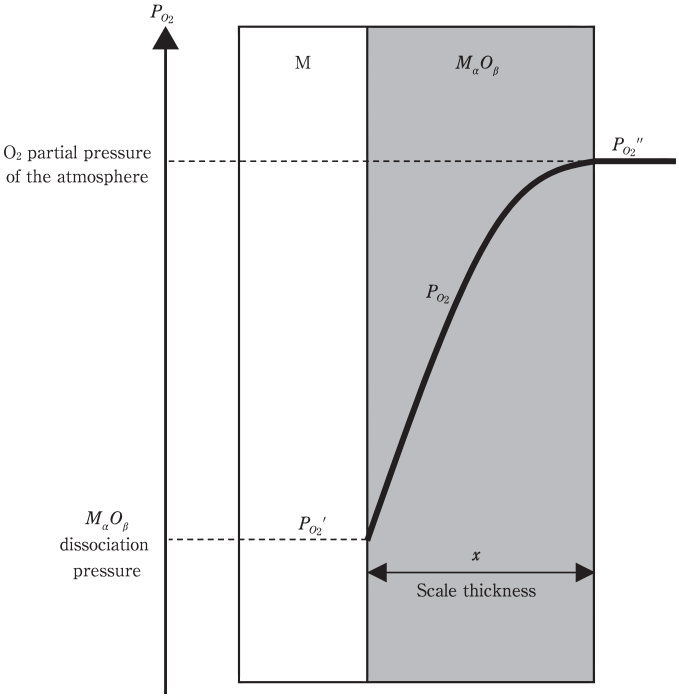


**Figure 10**
Diagram of how the partial pressure of a gas decreases inside a solid.

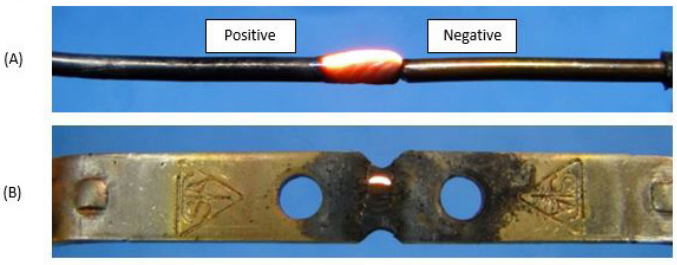


**Figure 11**
(A) shows a DC OPC where the liquid conducting worm only consumes the positive electrode. (B) shows a brass-to-brass OPC where the worm is shown to behave similarly to the other experiments. Metallurgical cross-sections of similar samples are documented in "Poor Electrical Connections: Physical Features, Materials Characterization, and Newly Identified Characteristic Traits, Before and After a Fire."

**Figure 11 (B)** shows the glowing worm between two brass plug blades with 2.2 amps of current flowing across the connection. The nominal circuit voltage is 120V AC, and the voltage drop across the connection was measured to be 7V.

In the examples studied in "Pre- and Post-Flashover Characteristics of an Electrically Overheated Poor Connection Between Copper and Steel"[2] and "Poor Electrical Connections: Physical Features, Materials Characterization, and Newly Identified Characteristic Traits, Before and After a Fire,"[3] it was also possible to identify the characteristics of the worm after samples were exposed to a fire environment. This was done primarily with metallography, though some features were still observable by surface examination.

## Case Study 1

This case involves a thermal cut out (TCO) switch from a commercial cooking range. The subject TCO, as shown in **Figure 12**, was presented to this author's laboratory by the range appliance manufacturer for a failure analysis. The subject TCO was part of a range that was being field tested under the control of the manufacturer. The range had been in service for approximately 10 months prior to the failure of the TCO crimp terminal connection. The current through the subject TCO is 20 amps during normal operation when both range heating elements are

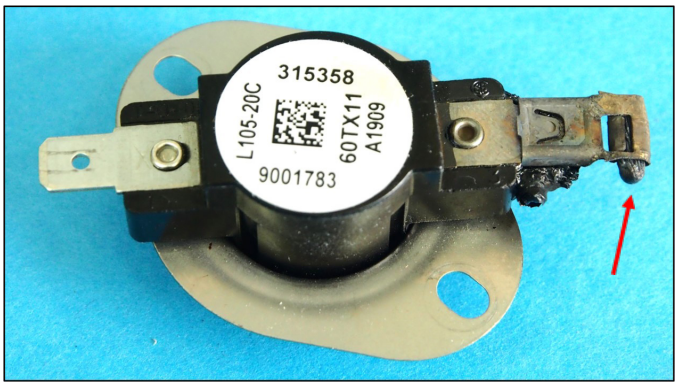


**Figure 12**
Subject TCO with overheated terminal crimp on the right-hand side. The TCO manufacturer markings have been blurred out.

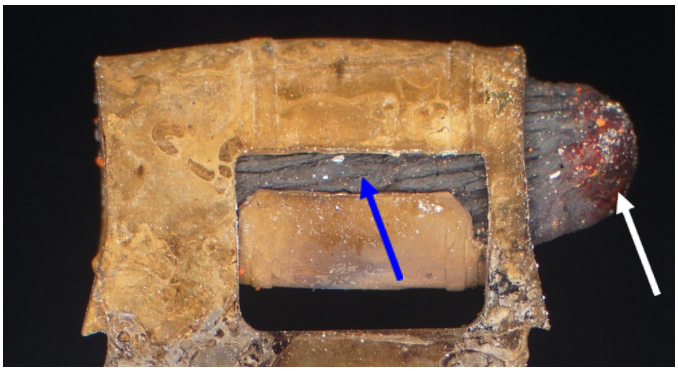

**Figure 13**
Digital image taken through the stereo microscope with crossed polarizing filters.

on. There is some melting and thermal decomposition of the plastic insulation materials close to the terminal, but no other surrounding materials ignited before the subject OPC melted open at the region indicated by the red arrow.

**Figure 13** shows a stereo microscope image of the subject crimp connection between the brass terminal and a stranded copper wire. This image was taken with crossed polarizing filters and the region where the stranded wire melted open is red colored, as indicated by the white arrow. The red color under crossed polarizing filters is consistent with $Cu_2O$ (cuprous oxide), which is semi-transparent and red colored under polarizing filters[11]. Also apparent is a gap in the crimp barrel, as indicated by the blue arrow.

**Figure 14** shows the subject crimp from the other side. It is clear there is a melted mass where the stranded wire once exited the crimp barrel, as indicated by the red arrow. The blue arrow points to localized melting of the female brass terminal body. In all the experiments performed by this author, where OPCs were produced in the lab under various conditions, essentially no evidence of melting was observed on the metallic conductors in the connection area. Yet, melting of the metallic conductor can occur for several reasons. The OPC may thermally degrade the surrounding materials such that parallel arc tracking across a carbonized path occurs between adjacent conductors.

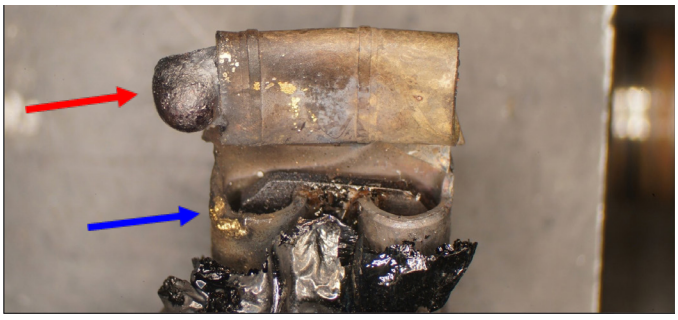

**Figure 14**
The red arrow points to the melted brass that formed after the subject circuit melted open. The blue arrow points to melting of the brass terminal body, which may have been caused by series arcing from contact with the stranded wire as it separated.

An OPC may cause parallel arcing if the insulation breakdown from the localized heating causes conductors to touch and short circuit. If an OPC ignites a fire, the fire may become hot enough to melt conductors. These aforementioned potential causes for melting do not appear to have caused the brass melting on the subject terminal. When the OPC melted open and severed, the stranded wire segment (not available for analysis) likely contacted the brass terminal body causing a 20-amp series arc and local melting. In general, circuits with higher amperage loads would be likelier to cause melting under series arcing conditions.

**Figure 15** shows the subject crimp at the end opposite the melted-open region. The subject crimp was improperly made because it failed to properly compress the copper strands, which can easily be seen by the large gaps between the strands. The copper strands themselves have undergone a significant amount of secondary high-temperature oxidation from the OPC. The red arrow points to a formerly liquid oxide mass, which, at some point, was undoubtably part of the molten worm. The rippled appearance, shiny gray exterior, and engulfed strands are a dead giveaway. Surface analysis of this worm region also shows micro-sized oxide spatter droplets. The blue

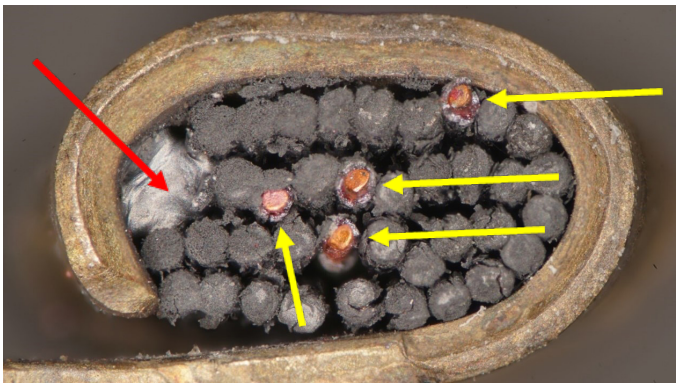

**Figure 15**
This shows a positive identification of an OPC worm between a brass crimp body and a stranded copper wire. This component had been installed in a real-world application, and the failure resulted in an open circuit. The red arrow points to a globular region, which was a worm at some point in time. The yellow arrows point to fractured high-temperature oxidation scale on the individual copper strands, which is a secondary effect of the heating caused by the worm. All of the wire strands not consumed by the worm globule display this secondary scale.

arrows point to the layer of high-temperature oxidation scale surrounding the copper strands.

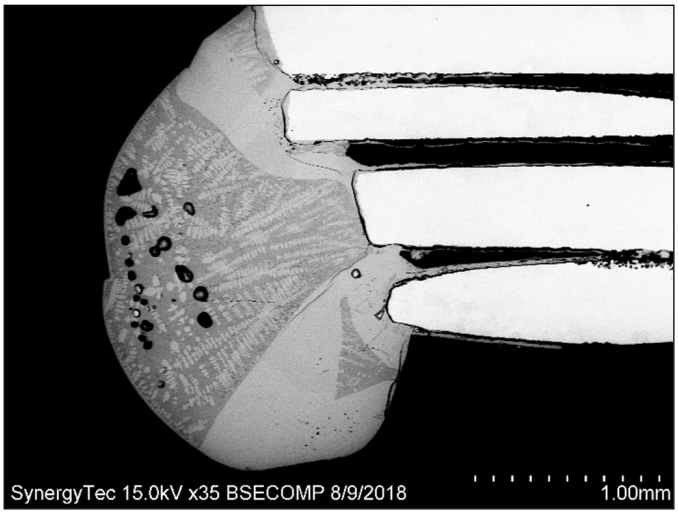


**Figure 16**
Above is an as-polished cross section[3] of a sample produced in the lab between copper electrodes with an AC current (2 amps for 20 minutes, then 13 amps for 20 minutes until the connection melted open).

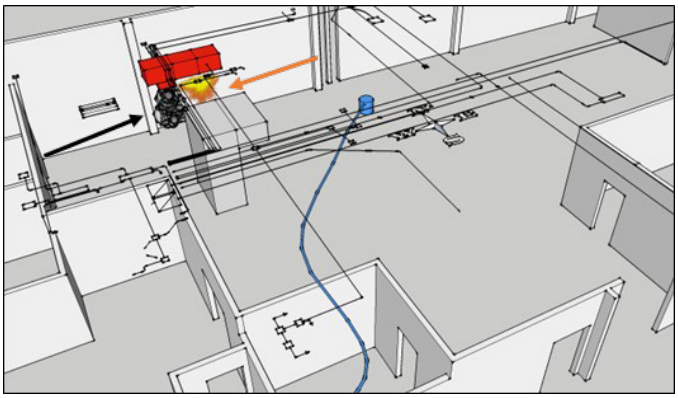

**Figure 17**
A model of the room where the fire took place. The blue wiring is the security camera and wiring; the red item is the furnace where the fire was first discovered. The furnace is above a drop ceiling.

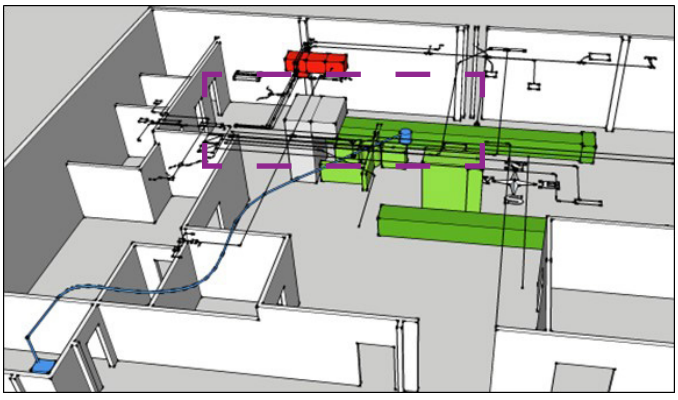

**Figure 18**
Macro view of the area identified by the plaintiffs as the origin, indicated by the dashed purple box.

**Figure 16** shows a polished cross-section of a solidified oxide mass from an experiment performed on a copper-to-copper OPC produced in the lab[3]. This sample ran with a current of 2 amps for 20 minutes (after which the circuit current was switched to 13 amps for 20 minutes), and the OPC proceeded to melt open. The last oxide liquid to solidify can be seen coming from one strand. It is expected the melted open cross-section (as shown in **Figure 11**) would display similar features if examined in similar detail.

## Case Study 2

A fire at a commercial bakery was the subject of an investigation led by a colleague of the author, who was hired by one of the defendants in a lawsuit and trial that followed. This defendant was an electrician who was working on an installation of a security camera system in the room of origin on the day of the fire.

The subject structure was used as a warehouse until 1998, after which the building was converted into a facility for pizza crust production. In the weeks prior to the fire, a video security system was being installed, which consisted of 16 cameras, two DVRs, and two power supply panels — each containing a power supply transformer. On the day prior to the fire, bakery maintenance personnel smelled overheating plastic in the room containing the camera power supply panels. The maintenance staff then shut off the circuit breakers serving these panels.

The following day, the defendant electrician discovered one of the camera power supply transformers had shorted and failed. He replaced the transformer, continued setting up camera circuits, and disconnected the camera circuits at the panels before leaving for the day. At least 4½ hours passed between the electrician leaving and the first smoke or fire observed by production workers.

**Figure 17** shows the location of where the first smoke and fire was observed by workers on the production line, as indicated by the black and orange arrows, respectively. The smoke was observed coming out of a return vent, and the first fire was seen about 7 feet from the return vent.

**Figure 18** shows a more zoomed out view of the subject structure compared to **Figure 17**. The production line in the room of fire origin is shown in green. The furnace where the first smoke and fire were observed is shown in red. This furnace was installed above a drop ceiling. The components shown in blue are a camera in the upper right, the power supply panel with the transformer is in the lower left, and the camera wiring is in between. The

region shown enclosed by the dotted purple box is the plaintiff's area of origin, which includes the camera/wiring and excludes the furnace. Other items in this region included a ceiling exhaust fan, fluorescent lighting, and associated wiring. The experts who were hired on behalf of the electrician defendant included the furnace in their area of origin and requested it be retained as evidence. This was based on the fire patterns in this area and the fact this was the location where smoke and fire were first witnessed.

At the first joint laboratory examination of the artifacts collected at the fire scene, the plaintiff's experts tested the transformer that had failed one day prior to the fire as well as the replacement to this transformer installed by the electrician defendant on the day of loss. The failed transformer, which was not in service on the day of loss, was found to have an open circuit in the primary windings. The transformer installed on the loss date exhibited no failure and was found to operate normally. At this exam, the expert on behalf of the electrician defendant requested the furnace and related components be examined further. The plaintiff's experts objected and concluded the joint exam.

Despite continued requests to examine the subject furnace, the plaintiff's experts maintained their objections. It was not until after the plaintiff's experts provided deposition testimony that additional examination of the furnace was found agreeable.

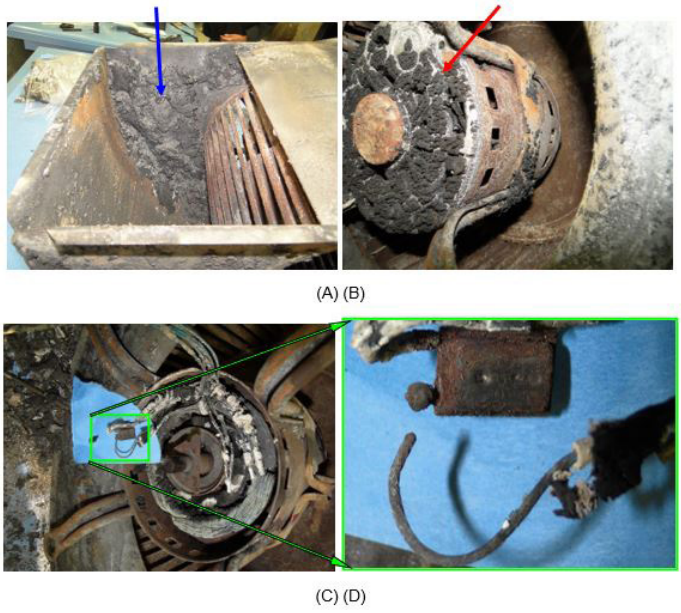


**Figure 19**
(A) shows caked-on flour deposits inside the blower volute, as indicated by the blue arrow. The witness who first spotted flames identified a location close to this component. (B) shows the motor end bell, which is caked with flour deposits. This is where the cooling fan within the motor housing draws in air to cool the motor. (C) is the thermal protector with the overheated connection, and (D) is a close-up of the melted open connection.

**Figure 19** shows four images from the subsequent examination of the furnace. (A) shows the furnace fan discharge with a thick layer of burnt flour deposits, as indicated by the blue arrow. (B) shows more burnt flour deposits on the end-bell of the motor for the furnace air handling fan, as indicated by the red arrow. (C) shows an image after the fan motor end-bell was removed, and (D) shows an enlarged view of the thermal protector switch, which exhibited a formerly molten bead consistent with an OPC and a solidified oxide that melted open. The stranded wire, which was previously crimped into the steel thermal protector body, also displayed localized melting consistent with an OPC.

**Figure 20** shows a close-up stereo microscope image of the formerly molten mass on the end of the subject motor thermal protector switch, as indicated by the blue arrow. This thermal protector employs a steel casing that carries the circuit current between the crimp connections and the interior contacts as well as the crimp connections. The other crimp connector is shown by the yellow arrow. Both of the subject crimp connectors are a copper to steel connection.

## Conclusions

For the conductor materials and circuit conditions studied, the liquid oxide conductor (aka worm) has been shown to be ubiquitous and identifiable. The phase diagram for the copper-oxygen system shows very clearly a region with

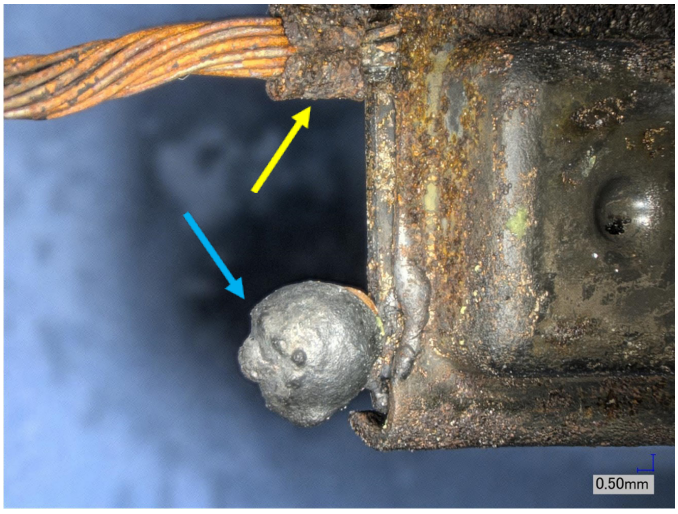


**Figure 20**
The blue arrow points to an oxide mass resulting from an OPC on the subject switch.

two immiscible liquids, which explains the microstructure of the conducting filament worm for Cu-Cu alternating current OPCs. Since the worm involves copper-rich particles, it would make sense that this is the favored electrical path. Given particles of copper dispersed in a matrix of $Cu_2O$, it would be expected that the electrical conductivity would follow the rule of mixtures as a first order approximation. This is another area for continued research. The conductivity measurements performed on Cu-Cu OPCs by others in the past deserve reconsideration in light of the fact that the material they were measuring was not monolithic CuO or $Cu_2O$, as in "Glowing Contact Physics."[4]

Other areas deserving more research have been identified in this paper, such as potential causes for metallic melting observed on materials involved in an OPC. Aspects of higher current OPCs that are expected to last for shorter time periods are under researched.

The first case study in this paper is a real-world example of an OPC from the field. This analysis shows some of the characteristic traits of an OPC, such as the worm traveling to the rear of the connection and creating an oxide mass that consumed several individual copper wire strands.

One major takeaway from Case Study 2 is never discount or ignore the witness accounts of where the smoke and fire were first observed.

## References

1. V. Babrauskus, *Electrical Fires and Explosions*, New York: Fire Science Publishers, 2021.

2. C. Korinek, T. Korinek and H. Lopez, "Pre- and Post-Flashover Characteristics of an Electrically Overheated Poor Connection Between Copper and Steel," in *Fire and Materials*, San Francisco, 2013.

3. C. Korinek and T. Korinek, "Poor Electrical Connections: Physical Features, Materials Characterization, and Newly Identified Characteristic Traits, Before and After a Fire," in *Fire Science and Technology* (ISFI), Chicago, 2018.

4. J. Shea, "Glowing Contact Physics," in *IEEE Holm Conference on Electrical Contacts*, Montreal, 2006.

5. *Principles of Electronic Materials and Devices*, New York: McGraw-Hill, 2006.

6. G. Garnaud, "The Formation of a Double Oxide Layer on Pure Copper," *Oxidation of Metals*, vol. 11, no. 3, 1977.

7. J. Shea and X. Zhou, "Material Effect on Glowing Contact Properties," in *IEEE Holm Conference*, 2007.

8. S. Bradford, Chapter on Fundamental of Corrosion in Gasses, Handbook Volume 13 - Corrosion, Materials Park, Ohio: ASM International, 1987.

9. *Properties and Selection: Nonferrous Alloys*, Materials Park, Ohio: ASM International, 1990.

10. M. Benfer and D. Gottuk, "Electrical Receptacles - Overheating, Arcing, and Melting," in *FIRE SAFETY SCIENCE*, 2014.

11. *Introduction to Practical Ore Microscopy*, 1989.

12. D. Shishin and S. Decterov, "Critical Assessment and Thermodynamic Modeling of the Cu–O and Cu–O–S Systems," *CALPHAD: Computer Coupling of Phase Diagrams and Thermochemistry*, vol. 38, pp. 59-70, 2012.

13. Y. A. Chang and K.-C. Hsieh, *Phase Diagrams of Ternary Copper-Oxygen-Metal Systems*, Materials Park, Ohio: ASM International, 1989.

14. E. Ehlers, *The Interpretation of Geological Phase Diagrams*, San Francisco: W. H. Freeman and Co., 1972.

15. M. Noguchi and H. Yakuwa, *Lecture on the Fundamental Aspects of High Temperature Corrosion and Corrosion Protection Part 1: Basic Theory*, 2016.

16. W. J. Meese and R. Beausolie, "Exploratory Study of Glowing Electrical Connections," NIST, Washington, D.C., 1977.